Title: The Genetic and Evolutionary Basis of Gene Expression Variation in East Africans

Authors: Derek E. Kelly[1,2], Shweta Ramdas[2], Rong Ma[3], Renata A. Rawlings-Goss[2], Gregory R. Grant[2], Alessia Ranciaro[2], Jibril B. Hirbo[4,5], William Beggs[2], Meredith Yeager[6], Stephen Chanock[7], Thomas B. Nyambo[8], Sabah A Omar[9], Dawit Wolde Meskel[10], Gurja Belay[10], Hongzhe Li[3], Christopher D. Brown[1,2], Sarah A. Tishkoff[2]*

Affiliations:

[1] University of Pennsylvania, Genomics and Computational Biology, Philadelphia, PA

[2] University of Pennsylvania, Genetics, Philadelphia, PA

[3] University of Pennsylvania, Biostatistics, Philadelphia, PA

[4] Department of Medicine, Division of Genetic Medicine, Vanderbilt University School of Medicine, Nashville, TN

[5] Vanderbilt Genetics Institute, Vanderbilt University Medical Center, Nashville, TN

[6] Frederick National Laboratory for Cancer Research, Frederick, MD

[7] National Institutes of Health, Division of Cancer Epidemiology and Genetics, Rockville, MD

[8] Department of Biochemistry, Kampala International University in Tanzania, Dar es Salaam, Tanzania

[9] Kenya Medical Research Institute, Center for Biotechnology Research and Development, Nairobi, Kenya

[10] Addis Ababa University, Microbial Cellular and Molecular Biology Department, Addis Ababa , Ethiopia

* Corresponding author

Abstract

Background: Mapping of quantitative trait loci (QTL) associated with molecular phenotypes is a powerful approach for identifying the genes and molecular mechanisms underlying human traits and diseases. How the genetic architecture of molecular traits varies across human populations, however, has been less explored. To better understand the genetics of gene regulation in East Africans, we perform expression and splicing QTL mapping in whole blood from a cohort of 162 diverse Africans from Ethiopia and Tanzania. We assess replication of these QTLs in cohorts of predominantly European ancestry and identify candidate genes under selection in human populations.

Results: We find the gene regulatory architecture of African and non-African populations is broadly shared, though there is a considerable amount of variation at individual loci across populations. Comparing our analyses to an equivalently sized cohort of European Americans, we find that QTL mapping in Africans improves the detection of expression QTLs and fine mapping of causal variation. Integrating our QTL scans with signatures of selection, we find several genes related to immunity and metabolism that are highly differentiated between Africans and non-Africans, as well as a gene associated with pigmentation, *TMEM216*, with evidence of population-specific selection in Nilo-Saharan speaking pastoralists.

Conclusion: Extending QTL-mapping studies beyond groups of European ancestry, particularly to diverse indigenous populations, is vital for a complete understanding of the genetic architecture of human traits and can reveal novel functional variation underlying human traits and disease.

Key Words: Human African genomics; gene expression; eQTL; human diversity; natural selection

Background

Gene regulation is a principal mechanism by which genetic variation contributes to phenotypic variation, making its study essential for understanding human evolution and disease. Nearly a half century ago, King and Wilson noted the high degree of conservation between the coding regions of humans and chimpanzees, positing that non-coding variation and its effect on gene regulation must account for much of the phenotypic divergence between these species [1]. The genomics era has further underscored the importance of noncoding variation in human disease and evolution: ~90% of the genotype-phenotype associations identified by genome-wide association studies (GWAS) cannot be explained by coding variation [2,3], and similarly, genomic regions harboring evidence of selection in humans are significantly more enriched for variants altering expression than protein coding [4].

While GWAS and scans of selection can identify genomic regions of interest, they often lack the resolution to identify the specific genes underlying traits or targeted by selection. To bridge this gap, studies have aimed to identify genetic variation associated with fine-scale, molecular phenotypes, through quantitative trait locus (QTL) mapping [5]. Combining these molecular QTL maps with GWAS through colocalization, transcriptome-wide association studies, or Mendelian randomization, continues to prove a fruitful approach for identifying genes causally linked to traits and potential drug targets. Unfortunately, there is a persistent ancestry bias in human genomics research, with nearly 80% of GWAS participants being of recent European ancestry [6,7], as well as the majority of participants of molecular trait studies [8], greatly limiting our ability to translate findings from GWAS to diverse populations, as well as discover population-specific variation of interest [9].

Recent studies have sought to address the genomics gap between groups of European and non-European ancestry, identifying novel GWAS associations and genetic variation contributing to gene expression differences across populations [10–14]. However, most global populations

continue to be understudied, particularly in sub-Saharan Africa. Africa is the birthplace of anatomically modern humans and harbors the greatest levels of human genetic diversity across continents. Africa is home to a large array of biomes and terrains, and indigenous Africans continue to practice diverse cultural and subsistence strategies. Together, these environmental pressures have driven remarkable adaptations to infectious disease [15], diet [16], and climate [11,17], often in a population-specific manner. These adaptive variants can have important implications for human health in Africa, and elsewhere [18], and Africa is therefore vital for our understanding of human evolutionary history and health.

In this study, we probe the genetic architecture of gene regulation in whole blood from indigenous East Africans by performing expression QTL (eQTL) and splicing QTL (sQTL) mapping in a cohort of 162 individuals, representing nine ethnic groups, from Ethiopia and Tanzania. We measure the degree to which African architecture is shared with that of non-Africans, test whether Africans harbor functional variation absent from existing cohorts, and investigate the demographic and genetic forces that may contribute to variation in gene regulatory architecture. We test whether fine-mapping of QTL signals is improved in Africans relative to an equivalently sized cohort of European Americans, and highlight individual genes with improved fine-mapping in Africans. Finally, we measure the effect of selective forces on shaping gene regulatory architecture and identify candidate genes under selection.

Results

Population Structure

The cohort for this study consists of 171 Ethiopian and Tanzanian individuals belonging to nine ethnically and culturally diverse sub-Saharan groups, including the Cushitic speaking Agaw and Weyto, the Semitic speaking Argoba and Amhara, the Omotic speaking Dizi, the Nilo-Saharan speaking Mursi, and the Chabu who speak an unclassified language similar to Nilo-

105 Saharan, and the Khoesan speaking Hadza and Sandawe (Figure 1A). These populations
106 practice a variety of subsistence strategies, including foraging (Hadza and Chabu currently,
107 Sandawe and Weyto formerly), with a diet diverse in foraged tubers, fruit, and hunted game;
108 pastoralism (Mursi), a lifestyle that revolves around cattle herding and a diet high in animal
109 proteins and fats; agriculturalism (Agaw, Amhara, and Argoba), a sedentary lifestyle with a diet
110 high in cultivated carbohydrates; and agropastoralism (Dizi), which relies on both crops and
111 livestock.
112
113 To investigate the genetic diversity and structure of these populations, a subset of 162
114 individuals were genotyped at approximately 4.5 million SNPs on the Illumina Omni5M Exome
115 array. These data were further imputed using a reference panel composed of the 1000
116 Genomes Project (1kGP) dataset [19] and a dataset of whole genome sequences (WGS) from
117 180 sub-Saharan African individuals (methods, unpublished). To place their genetic variation in
118 a global context, genotype data from the nine study populations were merged with 1kGP WGS
119 data from 20 individuals each of Yoruban (YRI), Northern and Western European (CEU), and
120 Han Chinese (CHB) ancestry (methods). Principal component analysis (PCA) of this merged
121 dataset recapitulates a primary separation between African and non-African individuals along
122 the first PC, explaining 3.8% of the variance. The second PC, explaining 1.8% of the variance,
123 further separates CEU and CHB individuals, as well as East Africans and the YRI (Figure 1B).
124 Higher PCs further separate variation in Africa; PC3 captures variation between the Hadza and
125 YRI, and PC4 between the Hadza and Chabu. Several groups cluster relatively nearer to CEU
126 Europeans along PC1, most notably the Ethiopian Agaw, Amhara, Argoba, and Weyto, which
127 are known to have moderate levels of Eurasian admixture [20,21]. Inferred ancestry
128 components from *ADMIXTURE* [22] also estimate components of non-African ancestry among
129 these Ethiopian groups, as well as admixture with Bantu-speaking populations of Western
130 African origin [19], represented by the YRI, in the Sandawe, Mursi, and Hadza (Figure 1C).

131

132 **Transcriptomic traits in Africans**

133 To assess the contribution of genetic variation to transcriptomic trait variation, we performed
134 genome-wide QTL mapping for expression (eQTL) and splicing (sQTL) transcriptomic traits in
135 *cis* for expressed protein-coding and long-noncoding RNA genes; collectively we will refer to
136 eQTLs and sQTLs as transcriptomic QTLs (tQTLs). We first correct our phenotypes (expression
137 and splicing) for a number of covariates, including age, sex, delivery date, hidden covariates
138 inferred by *PEER* [23], and cell-type fractions inferred by *CIBERSORT* [24]. Cell-type
139 composition of whole blood is known to vary between individuals, and to be a source of
140 confounding in QTL studies [25]. To account for ancestry and relatedness, we generate a
141 genetic relatedness matrix (GRM) and perform tQTL mapping using the linear mixed model tool
142 *GEMMA* [26]. Testing all autosomal SNPs with minor allele frequency (MAF) greater than 0.05
143 and within 100kb of the target gene transcription start site (TSS) for eQTLs or within 100kb of
144 the target intron for sQTLs, we identify 99,685 SNPs associated with the expression of 1,330
145 genes (eGenes) and 74,445 SNPs associated with splicing of 1,118 introns (sIntrons) in 776
146 genes (sGenes) at FDR < 0.05 (methods).

147

148 SNPs associated with expression (eSNPs) and splicing (sSNPs) show a characteristic
149 enrichment near the transcription start site or intron boundary of their target gene, respectively
150 [27] (Figure 2A), and are enriched in a variety of functional categories, including transcription
151 start sites, enhancers, and splice sites, and are depleted in repressed chromatin regions. We
152 also find a significant overlap with chromatin QTLs (caQTLs) identified in lymphoblastoid cell
153 lines (LCLs, Figure 2B). Further, alleles associated with increased chromatin accessibility are
154 significantly more likely to be associated with increased expression (OR = 2.9, $p = 8.2 \times 10^{-37}$
155 Fisher's Exact Test) and slightly less likely to be associated with increased junction inclusion
156 (OR = 0.82, p = 0.03 Fisher's Exact Test), suggesting that regulatory mechanisms altering

chromatin accessibility play a greater role in regulation of gene expression than splicing. When we restrict to variants with a greater than 10% probability of being causal (methods), we find a further enrichment in functional categories, particularly for caQTLs among eQTLs and splice regions among sQTLs, indicating we are capturing true causal variation (Figure 2B).

Of the genes tested, 198 have both an eQTL and sQTL in our cohort, suggesting possible shared genetic architecture between these transcriptomic traits. To evaluate whether eQTLs are enriched for sQTLs overall, we first compute the π_1 statistic, which measures the estimated fraction of sQTLs that are true positives in the eQTL scan. A π_1 value of 0.61 suggests that the majority of sQTLs affect expression or are in LD with variants affecting expression (Figure S3), though many of these fail to reach genome-wide significance. To further evaluate whether the genome-wide significant eQTL and sQTL signals are driven by shared causal variants, we estimated 90% credible sets for each set of QTLs, defined as the minimal set of variants which have at least a 90% probability of containing the causal variant, using the probabilities estimated above (methods). Overall we find overlapping credible sets for 114 of the genes with both a significant eQTL and sQTL, which makes up about 9% (114/1,330) of all eGenes in our cohort, comparable to the 12% overlap observed in GTEx [28]. Taken together, this observation suggests that splicing variants likely cause subtle but detectable changes in gene read counts, but that the genetic variants driving genome-wide significant eQTLs and sQTLs are largely independent.

Replication of tQTLs in non-Africans

To validate our tQTLs, and to assess sharing of molecular trait architecture between cohorts of predominantly African vs. predominantly European ancestry, we compared our results to whole blood analyses from the Genotype-Tissue Expression project (GTEx) v8, which is comprised of 85% European Americans [28]. For those QTLs tested in both cohorts, we find that both eQTLs

and sQTLs identified in the African cohort show overall high reproducibility in GTEx, with π_1 values for eQTLs and sQTLs of 0.88 and 0.90, respectively (Figure S4, methods). In addition to π_1, effect sizes between our cohort and GTEx also show overall strong concordance (Pearson's ρ = 0.73 for eQTLs and 0.82 for sQTLs, Figure 3: Replication of tQTLs between East Africans and GTEx v8). To assess whether the observed replication is significantly affected by the different genome versions used between our study and GTEx v8, we also measured π_1 of eQTLs in GTEx v7, finding a π_1 of 0.83 (Figure S4). Those tSNPs that fail to replicate in GTEx ($p > 0.01$) show consistently lower MAF (Figure 3: Replication of tQTLs between East Africans and GTEx v8); this failure to replicate includes the top eSNP in Africans for 308 genes and the top sSNP for 220 introns in 185 genes, indicating widespread differences in power for detecting tQTLs across ancestral groups.

We next investigate whether expression differences may affect replication between cohorts. Of the 1,330 eGenes identified in Africans, the expression of 98 in GTEx v8 whole blood is too low to be tested for eQTLs. These 98 genes are significantly enriched in two KEGG pathways, "Hypertrophic cardiomyopathy" (FDR = 0.032) and "Dilated cardiomyopathy" (FDR = 0.038). Investigating what may be driving broader expression differences for testable genes, we identify those genes measured in Africans that fail to reach expression thresholds for testing in GTEx whole blood and vice versa. Altogether 951 out of 12,377 genes measured in both cohorts and tested for eQTLs in Africans were not tested in GTEx. These genes are enriched for a number of biological processes related to sensory perception, including perception of smell (FDR = 2.85×10^{-6}), sound (FDR = 1.60×10^{-5}), mechanical stimulus (FDR = 5.60×10^{-5}), and chemical stimulus (FDR = 5.22×10^{-4}). Similarly, 6,728 out of 18,168 tested for eQTLs in GTEx were not tested in Africans and are enriched for several biological processes related to immunity, including "complement activation, classical pathway" (FDR = 1.78×10^{-22}), "humoral immune response mediated by circulating immunoglobulin" (FDR = 7.32×10^{-18}), and "B cell mediated

immunity" (FDR = 2.02 x 10^{-2}). This observation suggests that disease status, sample collection, and response to environmental factors, in addition to genetics, may account in part for incongruent findings between eQTL cohorts.

While tQTLs as a whole show strong replication using π_1, we also investigate the degree to which individual loci show evidence of shared causal variation. Estimating credible sets for all eGenes and sIntrons in GTEx v8 as described above, we find that 715/1262 (57%) of eGene credible sets and 619/852 (73%) of sIntron credible sets in Africans overlap with credible sets in GTEx v8. While the majority of tQTL credible sets overlap, the many non-overlapping sets suggests many tQTL signals identified in Africans may be driven by independent causal variants. To further evaluate this independence we remapped tQTLs in Africans, conditioning on sets of independent tQTLs identified in GTEx by forward regression [28]. In cases where there are no genome-wide significant eQTLs or sQTLs in GTEx (169 genes and 541 introns, respectively) we instead condition on the lead eSNP or sSNP in GTEx. Using the original FDR significance thresholds for calling eQTLs and sQTLs, we find that 362 (27%) of eGenes and 224 (20%) of sIntrons remain significant after conditioning on GTEx SNPs, including the top variants for 328 eGenes and 199 sIntrons, suggesting widespread independent causal variation in Africa.

Investigating what may be driving the independent signals in our cohort, we compare minor allele frequency (MAF), linkage-disequilibrium (LD) structure, and effect size differences between our cohort and GTEx v8 samples or European-ancestry proxies (CEU individuals from the 1kGP, methods). For 8 genes, *INPP5K*, *TMEM140*, *ACSM3*, *CNTNAP3*, *PPP1R14C*, *PDZK1TP1*, *GPR56*, and *TRAM2*, the top eSNP in Africans is untested in GTEx and has a MAF < 0.01 (the threshold used by GTEx) in 1kGP EUR populations. Similarly, the top sSNPs for 4 genes, *ADAM8*, *ICAM2*, *LINC00694*, and *MAPK1* are absent in GTEx and have a EUR MAF ≤

0.01. Overall, however, we find that frequency differences between Africans and EUR are similar between shared and independent tQTLs (Figure S6). To investigate the impact of LD variation on tQTL replication, we estimate r^2 between tQTL lead SNPs and SNPs within 100kb of lead SNPs in 1kGP CEU and YRI populations. We find that correlations between CEU and YRI r^2 values do not differ significantly between shared and independent tQTLs (Figure S6). Finally, comparing effect size variation, we find a significant reduction in effect size correlation between Africans and GTEx among independent tQTLs relative to shared signals (Figure 3: Replication of tQTLs between East Africans and GTEx v8, $p < 2.2 \times 10^{-16}$), which may reflect true effect size variation, GxE effects [13,14,29], or possibly more subtle differences in MAF and local LD between these cohorts [30].

Fine Mapping

In addition to assessing the replication of transcriptional QTLs in the larger GTEx v8 dataset, we are interested in the relative power to detect and fine-map tQTLs between cohorts of predominantly African versus European ancestry. To account for sample size differences between our cohort and GTEx, we performed eQTL mapping in a size-matched sample of 162 European-American (EA) individuals from GTEx v8 using *FastQTL* [31], with sex, sequencing platform, PCR batch, the top 15 *PEER* factors, and top 5 genotype PCs as covariates. Testing all SNPs with MAF > 0.05 within 100kb of the target TSS, we identify 1,029 eGenes in the 162 EA individuals at FDR < 0.05, compared with 1,330 identified in Africans, of which 326 eGenes are FDR-significant in both cohorts. Despite only 326 eGenes being shared, we find consistently high replication in an independent whole blood meta-analysis [32]; eQTLs that are FDR-significant in both cohorts reach a π_1 of 0.999, while eQTLs discovered only in Africans reach a π_1 of 0.958 and eQTLs discovered only in EAs reach a π_1 of 0.989. This observation suggests that the greater number of eGenes in Africans is not driven by an increase in false positives,

and that at similar sample sizes, Africans have an improved power to detect eQTLs compared with individuals of European ancestry.

We next investigate the relative ability to fine-map eQTLs between our African cohort and the 162 EA individuals from GTEx v8. Considering eGenes that are FDR-significant in either cohort (methods), we perform fine-mapping in both our African cohort and the 162 EAs using the approach described above. Overall, most genes do not fine-map well at this modest sample size, with 57% of genes having a credible set larger than 50 in both cohorts (Figure 4: Fine mapping in East Africans vs. GTEx v8). Excluding these genes, we find that Africans have a smaller credible set in 63% of cases (437/697, $p = 2.06 \times 10^{-11}$ binomial test), with a median credible set size of 25 in Africans vs 58 in EAs, and 23 genes fine-mapped to a single variant in Africans vs. 13 in EAs. One possible explanation of the smaller credible sets in Africans is that Africans simply have fewer SNPs tested per gene; however, we find the opposite, with 94% of genes have fewer tested SNPs in EAs.

We further compare our credible sets in African eQTLs to credible sets estimated in the full GTEx dataset. As expected, the majority of genes have smaller credible sets in GTEx due to the considerably larger sample size (670 vs 162), though we do identify several examples of greatly reduced credible sets in the African cohort. For 18 eGenes and 32 sGenes we are able to fine-map the QTL signals to a single variant in Africans and find that these variants overlap a lead GWAS association for 10 eGenes and 3 sGenes (supplement). We highlight rs883871 (Figure 4: Fine mapping in East Africans vs. GTEx v8), an eQTL for both *THRA* and *NR1B1*, which is FDR-significant in GTEx whole blood but is not the lead eSNP. rs883871 is a strong chromatin QTL in lymphoblastoid cell lines (LCLs) [33], overlaps the binding sites of numerous transcription factors (TFs) in the LCL GM12787 [34], is predicted to disrupt a consensus motif for the ETS family of TFs, which share a core ‘CCGGAA’ motif, and is the lead SNP for a

Multiple Sclerosis GWAS association [35]; variants in *ETS1* itself have been previously associated with Multiple Sclerosis [36]. Given our modest sample size compared with GTEx, we expect that mapping of tQTLs and other molecular traits in larger cohorts of genetically diverse populations will further enhance fine-mapping of QTLs, and when combined with more diverse GWAS studies, may identify novel causal genes underlying human traits and disease.

Signatures of Selection

Gene regulation is known or suspected to underlie many adaptive traits in humans, including diet [16,37], immunity [38], and skin pigmentation [11], and transcriptomic traits show evidence of both purifying and positive selection [13,14,39]. Consistent with previous tQTL studies we find decreasing effect size with increasing MAF among eQTLs and sQTLs, indicative of negative selection against variants of large effects (Figure S7). To identify QTLs with evidence of positive selection we measure genome-wide F_{ST} between our broader African dataset and the 1kGP European (EUR) individuals, with the expectation that selection for expression-altering alleles will lead to increased differentiation at these loci. To assess whether tQTLs are enriched for evidence of positive selection we identify the highest F_{ST} value for all SNPs in high LD ($r^2 > 0.8$) with the top eQTL or sQTL and compare these values with null SNPs matched on MAF and the number of SNPs in LD (methods). Overall, we do not find an enrichment of high F_{ST} among eQTLs or sQTLs, suggesting that selection has not driven significant frequency differentiation at the majority of tQTLs (Figure S8).

We next investigate evidence of selection at individual loci. To account for the fact that the top eSNP may not be the true causal SNP, we score an individual gene's evidence of selection by taking a weighted sum of each SNP's F_{ST} value multiplied by the probability of that SNP being causal (methods). Considering loci with a score within the 99th percentile threshold of all SNP F_{ST} values as candidates, we identify 27 eGenes and 25 sGenes with evidence of selection

(supplement). The most differentiated eGene is *TTC26* (weighted F_{ST} = 0.59); a mutation in this gene has been associated with abnormal cilia in model organisms and biliary ciliopathy in human liver [40]. We also identified a strong signature of selection at *TMEM154* (weighted F_{ST} = 0.59, Figure 5A), a mostly uncharacterized gene that has been associated with Type II Diabetes Mellitus and beta cell function in humans and lentiviral infection in sheep [41,42]. Other highly differentiated loci include Platelet Factor 4 Variant 1 (*PF4V1*, F_{ST} = 0.50), *IL8* (F_{ST} = 0.49), a major inductor of immune cell chemotaxis and activation [43], and *CCR1* (F_{ST} = 0.43), a chemokine receptor. Among the most differentiated sGenes we find several related to immunity and metabolism, including *NADSYN1* (weighted F_{ST} = 0.50), a gene associated with vitamin D concentration [44], *BTN3A3* (weighted F_{ST} = 0.50), a butyrophilin gene implicated in activation of T cells [45], and *GANC* (weighted F_{ST} = 0.43), a member of the glycosyl hydrolase family 31, which play a key role in glycogen metabolism [46].

Given our genetically and culturally diverse cohort we are also interested in tQTLs with evidence of population-specific differentiation and selection. For each of the nine populations in the African dataset we calculate a modified version of the *d* statistic [47], a summation of normalized, pairwise F_{ST}, which tests for variants that are highly differentiated in a focal population versus other populations (methods). As above, we weight these *d*-statistics by the probability of a SNP being causal to derive a '*d*-score' for each gene or intron. Genes with high *d*-scores in populations with evidence of non-African admixture (i.e. Agaw, Amhara, Argoba, and Weyto) are more genetically similar to EUR samples from the 1kGP, based on F_{ST}. Conversely, populations with evidence of west-African admixture (i.e. the Hadza, Mursi, and Sandawe) are more genetically similar to YRI samples at high *d*-score genes, suggesting that in many cases the genetic differentiation at these loci is driven by population-specific patterns of admixture. We therefore calculate the population branch statistic between (*PBS*) [48] between individual populations in our study and 1kGP CEU and YRI populations. Considering genes with

a weighted *d* and *PBS* score in the top 99.5th percentile as significant, we identify 22 eGenes and 22 sGenes with significant evidence of population-specific selection (Figure 5: Population-specific selection in East Africa. and B).

Among the top eGenes with evidence of population-specific selection is *TMEM216* among the Nilo-Saharan speaking Mursi pastoralists (Figure S9). This gene is located near a skin pigmentation GWAS locus discovered in a cohort with the same sub-Saharan African populations [11]. This association signal overlaps the UV-repair gene *DDB1*, as well as several other genes expressed in melanocytes. Colocalization analyses show strong overlap between the African *TMEM216* eQTL and pigmentation GWAS signals (PP4 = 0.95, Figure 5C, methods), suggesting possible shared causal variation between *TMEM216* expression and pigmentation variation. LD patterns around *TMEM216* shows evidence of three independent eQTLs segregating for this gene, tagged by rs7948623, rs11230664, and rs3741265. Two of these SNPs, rs7948623, rs11230664, are also genome-wide significant GWAS SNPs for pigmentation variation in Africans, while the third, rs3741265, is marginally significant ($p < 10^{-5}$, Figure 5C), All three SNPs show strong population-specific differentiation in Ethiopian Nilo-Saharan groups, who have amongst the highest levels of skin melanin of any global population (Figure S9). Previous analyses of these populations have shown evidence of a selective sweep near this pigmentation GWAS locus, including high *PBS* and *d* values among GWAS variants (Figure S10) and extreme negative Tajima's D values overlapping the *TMEM138/TMEM216* locus [11].

The top GWAS variant, rs7948623, overlaps an active enhancer in keratinocytes and melanocytes and has been demonstrated to alter enhancer activity in melanocytes via luciferase reporter assays [11]. rs7948623 is a significant eQTL for *TMEM216* in our study but is not significant in GTEx whole blood, though it is in ovary, nerve, and exposed skin. In addition,

rs7948623 is a significant sQTL for *TMEM216* in multiple GTEx tissues, including exposed skin (Figure 5C). A second group of *TMEM216* eQTL and pigmentation GWAS variants are tagged by rs11230664 and include the indel rs148172827, which overlaps an active melanocyte enhancer, and shows significant correlation with *TMEM216* expression in GTEx exposed skin (Figure 5C). We do not identify significant sQTLs in Africans for *TMEM216*, however the top sSNP for *TMEM216* in GTEx exposed skin, rs3741265 ($p = 1.43 \times 10^{-322}$), is in high LD with the top TMEM16 eQTL in Africans, rs7934229 ($r^2 = 0.99$). Both of these SNPs are moderately associated with skin pigmentation in Africans ($p < 5 \times 10^{-6}$) but do not reach genome-wide significance (Figure S11).

Discussion

This study extends our understanding of the genetic basis of human gene regulation, with the inclusion of whole blood samples for 162 ethnically diverse sub-Saharan Africans from Ethiopia and Tanzania. We find that variation underlying expression and splicing is broadly shared between African and European cohorts, though there is considerable independent variation at individual loci in Africans, often driven by variation in frequency and effect sizes of tQTLs. When matched for sample size, Africans show improved fine mapping of molecular traits, facilitating the identification of causal variants and candidate genes underlying GWAS traits. This diverse cohort also allows for inference of tQTLs with evidence of local adaptation, identifying *TMEM216* as a target of selection in Nilo-Saharan speakers and a candidate gene that may play a role in skin pigmentation.

We find that the majority of tQTLs replicate between Africans and GTEx v8, with π_1 values near 0.9 among both eQTLs and sQTLs, on par with the 0.919 value estimated between African Americans in the GENOA cohort [49] and EUR populations from the Geuvadis project [12]. We also observe strong effect size correlation between tQTLs in our study and GTEx v8.

Investigating individual loci, however, we find that many genome-wide signals are driven by distinct causal variation; 43% of eQTL and 27% of sQTL credible sets in Africans do not overlap those in GTEx v8, and 27% of eGenes and 20% of sIntrons have QTL signals that remain significant after conditioning on all tGTLs in GTEx.

Investigating what may account for QTL differences between Africans and non-Africans, we find that genes relating to sensory perception and immunity show differential expression between our African cohort and the GTEx cohorts, pathways known to vary across populations and environments [50,51]. Additionally, the post-mortem nature of GTEx samples may contribute to expression differences. An analysis of the effects of death on gene expression in GTEx found that immune genes in whole blood are significantly dysregulated following death, however this change was characterized by an overall deactivation of immune genes, along with an overall increase in NK cells and CD8 T-cells and a reduction in neutrophils [52]. In addition to expression differences, we find an enrichment for low frequency variants in GTEx among non-replicating tQTLs. However, the majority of tQTLs that are conditionally independent show similar frequency differences with shared tQTLs, suggesting that frequency variation alone cannot account for independent tQTLs. This issue of trans-ethnic GWAS replication is an ongoing area of research [53,54], and non-replication may occur for many reasons including frequency variation, differences in power, LD, or true differences in effect size, including G x E effects. While we do not find a significant difference in local LD structure between shared and independent QTL signals, we do find significant differences in estimated effect sizes. Using a Bayesian approach to account for frequency and LD variation, Brown *et al*. also found eQTL effect size differences between EUR and YRI individuals from Geuvadis [12], which become more pronounced as genetic effects become weaker [55]. However for strong, genome-wide significant effects, Zanetti and Weale demonstrated using simulations that most trans-ethnic

differences in GWAS effect sizes can largely be accounted for by a combination of frequency and LD variation, though they could not rule out effect size differences [30].

Beyond replication, we demonstrate that at comparable sample sizes, African cohorts have improved sensitivity to detect tQTLs and improved ability to fine-map causal variants, compared with cohorts of European ancestry. It is well established that non-African populations have more extensive LD relative to Africans [56,57], resulting from the out-of-Africa bottleneck [58,59], which likely accounts for the observed improvement in fine-mapping in African populations. As to the increased sensitivity to detect tQTLs in Africans, one hypothesis is a higher false-positive rate in the African cohort. However we find comparable replication of African-specific tQTLs in a large, independent meta-analysis [32], suggesting that false positives do not account for the observed improvement. Moreover, Quach *et al.* found a similar pattern of improved sensitivity to detect eQTLs in individuals of self-reported African ancestry in an analysis of stimulated and unstimulated monocytes from 200 Belgians, 100 of European and 100 of African ancestry [60]. Among African Belgians they found 13% more eQTLs in unstimulated monocytes, and 10% more eQTLs across all conditions. While several other studies have mapped eQTLs across multiple ancestry groups [12,14,61,62], variation in sample size precludes direct comparison of sensitivities across ethnicities.

In addition to the inclusion in our study of ancestral groups not represented in existing reference cohorts (e.g. the 1kGP), which enables the detection of novel regulatory variation, these populations live in diverse climates and have distinct cultural and subsistence practices, which may have driven unique local adaptations. Using an outlier approach based on the F_{ST} based *d* and *PBS* statistics [47,48], we identify population-specific differentiation of tQTLs among East African populations. One notable example is the eQTL *TMEM216* among the Mursi, which is near a recently identified pigmentation locus specific to sub-Saharan Africans [11]. *TMEM216,*

and the nearby *TMEM138* gene, form an evolutionarily conserved *cis*-regulatory module vital for ciliogenesis, and have been identified as causal genes underlying Joubert and Merkel syndromes [63,64]. *TMEM216* has not been previously associated with pigmentation variation, though activation and suppression of primary cilia have been shown to inhibit and activate melanogenesis, respectively, in a human skin model [65]. Consistent with this, we find that the expression decreasing allele is associated with increased melanin levels for rs7948623, rs11230664, and rs3741265, and is most common in the Mursi, a populations with darkly pigmented skin (Figure S9)[11]. In addition, recurrent somatic mutations driving alternative splicing of *TMEM216* are significantly associated with melanoma in The Cancer Genome Atlas (TCGA), suggesting possible tumor suppressor function for this gene [66]. While the strong colocalization between the *TMEM216* eQTL and pigmentation GWAS signals suggests *TMEM216 as* a possible pigmentation gene, there are several haplotypes segregating in this region, some of which carry tQTLs for other genes in GTEx (Figures S12 and S13). In addition, several nearby genes show melanocyte-specific expression, or have been previously associated with pigmentation in other organisms, complicating identification of the gene or genes that are causally associated with pigmentation variation [11,67].

There are several limitations to our study, foremost being our modest sample size of 162 individuals, with current eQTL datasets reaching sample sizes an order of magnitude larger [49]. Many of the populations participating in this study live at considerable distances from medical or scientific facilities, and all necessary tools and supplies must be transported to field sites, greatly limiting the capacity for sample collection. Additionally, we are limited to studying blood tissues among these populations. Generation of induced pluripotent stem cells (iPSC) may allow for the study of gene regulation across developing tissues or differentiated cells within diverse populations [68,69], but such approaches remain technically difficult. This study is also restricted to steady state gene expression, which may miss cell-type- or dynamic, environment-

specific genetic effects, which cannot be captured in bulk and/or steady-state tissues [29,70,14,13,71,72]. Despite these limitations, this study makes important contributions to our understanding of gene expression variation and the molecular basis of human adaptation in sub-Saharan Africa.

Conclusion

We have presented a comprehensive analysis of transcriptomic variation in a cohort of previously unstudied indigenous sub-Saharan Africans. We identify extensive novel regulatory variation in Africans and show that the study of African populations improves the detection of transcriptomic QTLs and fine mapping of causal variation. Studying diverse populations within Africa also allows for the detection of genes targeted by population-specific selection, including a evidence of selection on *TMEM216* expression in the Mursi and strong colocalization between *TMEM216* eQTLs and a pigmentation GWAS locus.

Methods

Sample Collection

Phenotypic, genealogical, and biological data were collected from individuals belonging to nine populations in Ethiopia and Tanzania. Prior to sample collection, IRB approval for this project was obtained from the University of Pennsylvania. Written informed consent was obtained from all participants and research/ethics approval and permits were obtained from the following institutions prior to sample collection: the University of Addis Ababa and the Federal Democratic Republic of Ethiopia Ministry of Science and Technology National Health Research Ethics Review Committee; COSTECH, NIMR and Muhimbili University of Health and Allied Sciences in Dar es Salaam, Tanzania. To obtain DNA and RNA data, whole blood was collected using vacutainers and RNA was stabilized in the field using LeukoLOCK Total RNA Isolation System (Ambion life Technologies). The Poly(A)Purist Kit (Ambion Life Technologies, CA) was used for

493 mRNA selection, and Ampure XP magnetic beads (Beckman Coulter, CA) were used for size
494 selection after amplification.
495
496 **Genotyping and imputation**
497 A subset 162 individuals were genotyped as part of the 5M dataset using the Illumina Omni5M
498 SNP array, which includes approximately 4.5 million SNPs. The full 5M dataset was phased
499 using Beagle 4.0 [73] and the 1kGP reference panel [19]. These data were further imputed
500 using minimac3 [74] and a reference panel consisting of the 1kGP and 180 WGS from the
501 Tishkoff lab (unpublished).
502
503 **PCA and ADMIXTURE**
504 To identify related individuals, relatedness was inferred in the imputed 5M dataset using the
505 KING extension of plink 2.0 [75]. To place the genetic variation in this study within a global
506 context, the 5M imputed dataset was merged with the 1KGP. Individuals from the 162 in this
507 study with inferred relatedness more distant than third degree were then extracted from the
508 merged dataset (145 total), along with 20 individuals each from the YRI, CEU, and CHB
509 populations, restricting to unambiguous SNPs (i.e. excluding A/T and C/G) with MAF > 0.01 and
510 with imputation accuracy (r^2) greater than 0.99 reported from minimac3. SNPs were LD-pruned
511 using plink v1.90 [76] and parameters '--indep-pairwise 50 10 0.1'. PCA was performed on this
512 dataset using smartpca from EIGENSOFT v6.1.4 [77], with 'numoutlieriter' set to 0.
513 ADMIXTURE [78] was run on the same dataset using parameters '--cv -j8 -B100 -s7'.
514
515 **mRNA sequencing and molecular trait quantification**
516 Samples were sequenced on an Illumina HiSeq to a median depth of 56,122,076 reads
517 (11,727,716 min., 228,660,534 max.). Prior to mapping, all reads aligned to rRNA genes with
518 BLAST [79] were removed. Remaining reads were mapped to the hg19 genome with STAR

v2.5.3a [80] and the GTEx GENCODE v19 gene annotations [81] using two-pass mapping. Expression was quantified at the gene level using featureCounts v1.5.3 [82] as fragments per gene, as well as using RSEM v1.2.31 [83] as transcripts per million (TPM). Splicing was quantified using leafcutter [84] as fraction of intron exclusion reads per cluster (JPC).

Cell-type inference

Cell type fractions for each individual were inferred using CIBERSORT [24]. The LM22 signature gene file from Abbas *et al*. [85] was used to infer frequencies of 22 immune cell types for a mixture file of TPM values for all 171 individuals with RNA-seq data. Quantile-normalization was disabled and 1000 permutations were used.

Quantile normalization and hidden factor inference

Prior to hidden factor inference and QTL mapping, molecular phenotype matrices were first filtered and quantile-normalized. For eQTL mapping, only lncRNA and protein-coding genes with more than 5 reads in at least 20 individuals and with mean TPM > 0.1 across all populations were considered. For sQTL mapping, introns from lncRNA and protein-coding genes with no more than 5 individuals with 0 reads were included. Furthermore, clusters were required to have at least 20 reads in at least 100 individuals and have 0 reads in fewer than 10 individuals. These filtered phenotype matrices (TPM for eQTL mapping and JPC for sQTL) were then quantile normalized using the two-stage procedure implemented by GTEx [28]. Briefly, the distribution of the phenotypes per individual were first quantile normalized to the mean of the phenotypes across individuals. Next, the distribution of each phenotype was quantile normalized to the standard normal. Hidden covariates were inferred using *PEER* [23] for these quantile-normalized phenotype matrices.

eQTL and sQTL mapping

Expression and splicing quantitative trait loci were mapped using a linear mixed modelling approach, using the quantile-normalized gene or intron fractions as phenotypes, while correcting for sex, age, cell-type composition, delivery date, latent *PEER* factors, and genetic relatedness. Mapping was performed for SNPs with MAF > 0.05, imputation $r^2 > 0.3$, and within 100kb of the target phenotype (gene TSS for eQTLs and intron for sQTLs) using *GEMMA* [26] and a genetic relatedness matrix (GRM) generated from all biallelic SNPs across the imputed, 162 individual genotype dataset. tQTL mapping was repeated across a range of *PEER* factors: 0-5, 10, 15, 20, 25, and 30 factors for eQTL mapping, and 0-10 factors for sQTL mapping, and the number of factors maximizing the number of eQTLs or sQTLs discovered were chosen for downstream analysis.

To identify significant QTLs, tested SNPs for each phenotype were first FDR corrected using Benjamini-Hochberg (BH), yielding single-corrected p-values (*P'*) for each tested SNP-phenotype pair. The minimum *P'* per phenotype were again FDR-corrected using BH, yielding double-corrected p-values (*P''*) per phenotype, and phenotypes with *P''* < 0.05 were considered significant. To identify significant SNPs, a threshold was set equal to the lowest *P'* for the phenotype with highest significant *P''*, and all SNPs with *P'* lower than this threshold were deemed significant.

Credible Sets

For each gene or intron of interest, Approximate Bayes Factors were calculated for each tested SNP using the function 'approx.bf.estimates' from the coloc package [86], or the function 'approx.bf.p' in cases where effect size or standard error information was not available. The posterior probability of each SNP *n* being causal (PP_n) was then taken as:

$$PP_n = \frac{ABF_n}{\sum_p ABF_p}$$

Similar to The Wellcome Trust Case Control Consortium *et al.* [87], where ABF_n is the Approximate Bayes Factor of SNP n, and p indexes all tested SNPs for a given feature of interest. A 90% credible set was then defined as the minimal number of SNPs whose sum of posterior probabilities was > 0.9.

Functional Enrichment

All SNPs in the imputed genotype dataset of 162 individuals were annotated for functional consequences using the Variant Effect Predictor (VEP) [88] with parameters '--per_gene --most_severe'. In addition, SNPs were overlapped with 15 state ChromHMM tracks for PBMCs (E062) from the Roadmap Epigenomics Consortium [67], transcription factor binding sites for lymphoblastoid cell lines (LCLs, GM12878) from ENCODE[34], and chromatin QTLs from Tehranchi *et al*. [33]. To test for enrichment, each FDR-significant eQTL or sQTL was matched on MAF and distance to nearest TSS or intron boundary, respectively, and the log-ratio of tQTL SNPs to matched background SNPs overlapping each functional category was taken as an enrichment score. This was repeated 10,000 times, producing an empirical distribution of enrichment scores for each functional category.

Replication with GTEx v8

All SNPs and intron boundaries were converted to hg38 coordinates using liftOver [89]. For eQTLs, those hg19 SNPs that successfully mapped to locations in hg38 (81,928/82,144) and genes with Ensembl IDs shared between GENCODE v19 and GENCODE v26 (1,291/1,330) were considered (96,903/99,685 of possible eQTLs). Of these, 77,238 eQTLs were tested in GTEx v8 and could be compared. For sQTLs, SNPs and Ensembl IDs were required to successfully map between versions (49,706/49,794 and 772/776, respectively), and intron boundaries were required to map between GENCODE versions (738/1,118). Of these, 55,046

sQTLs were tested in GTEx. The fraction of true positives for successfully mapped tQTLs in GTEx, π_1, was estimated using the R package *qvalue* [90].

Conditional tQTL mapping

To identify tQTLs in the African cohort that are independent of GTEx v8 tQTLs, we performed eQTL and sQTL scans conditioning on independent GTEx eQTLs and sQTLs identified via step-wise regression [91]. In cases where there are no significant tQTLs in GTEx we instead use the top variant per feature. To account for these variants, we residualize the quantile-normalized feature matrices used in the original QTL mapping against the genotypes of independent GTEx QTLs. We then perform identical eQTL and sQTL scans, and consider genes and introns with variants that pass the original FDR threshold as independent.

LD variation across populations

To compare LD structure between East Africans and Europeans at tQTL loci, LD was estimated (using r^2) between lead SNPs for eQTLs and sQTLs and all tested SNPs in the East African and 1kGP EUR samples, restricting to those variants polymorphic in both, resulting in an r^2 vector per group (East Africans and EUR) per locus (eGenes and sIntrons). For each tQTL locus, we estimated the Pearson correlation ρ between the East African and EUR r^2 vectors, and the distribution of these ρ values was compared for tQTLs shared between East Africans and GTEx and independent tQTLs.

eQTL mapping in 162 European-Americans from GTEx v8

eQTL mapping was performed on 162 individuals of European ancestry from GTEx v8 using FastQTL [31] with 10,000 permutations for all SNPs with MAF > 0.05 and within 100kb of the target TSS. Covariates included the top 15 *PEER* factors, top 5 genotype PCs, sex, platform,

and PCR batch. Significance was evaluated using the hierarchical Benjamini-Hochberg procedure used for African samples.

Scans of selection

To test for genetic differentiation between our African dataset and Europeans, all individuals belonging to the 9 populations in our study were extracted from the full 5M dataset (664 total) and allele frequencies were combined with frequency information for EUR populations from the 1KGP, restricting to SNPs polymorphic in both datasets. F_{ST} was estimated using the Hudson estimator [92], and SNPs within the top 99th percentile (F_{ST} > 0.36) were considered outliers. To test for overall enrichment of F_{ST} outliers among tQTLs, we use an approach similar to Quach *et al.* [13] The maximum F_{ST} value of SNPs in LD with lead tQTL SNPs (r^2 > 0.8) was found, and the fraction of outliers among these maximum F_{ST} values was calculated. To generate a null expectation, each lead tSNP was matched with a random SNP, matching on MAF (bins of 0.05) and number of SNPs in LD (bins of [0], [1], [2], (2,5], (5,10], (10,20], (20,50], and >50). The maximum F_{ST} of SNPs in LD with these matched SNPs was found, and the fraction of outliers among these matched maximum F_{ST} SNPs calculated. This procedure was repeated 10,000 times, generating a null distribution of expected number of outlier SNPs.

To identify individual eGenes and sGenes with evidence of selection, weighted F_{ST} scores were generated for each eGene and sIntron. For each feature of interest (gene or intron), the posterior probability of each tested SNP was calculated using the approach used to define credible sets, and for each feature a weighted F_{ST} score was calculated as:

$$\overline{F_{ST}} = \sum_{p} PP_p \; F_{ST}^{p}$$

Where PP_p is the posterior probability of SNP p being causal and F_{ST}^{p} is the F_{ST} of SNP p. Scores higher than the 99th percentile of genome-wide F_{ST} values were considered significant.

643

644 To detect population-specific selection, we use an adapted, polarized version of the *d* statistic
645 for each SNP:

$$d_i = \left| \sum_{j \neq i} \boldsymbol{I}_{p_i \geq p_j} \frac{F_{ST}^{ij} - E\left[F_{ST}^{ij}\right]}{sd\left[F_{ST}^{ij}\right]} \right|$$

646 Where p_i and p_j are the allele frequencies in populations i and j, respectively, $\boldsymbol{I}_{p_i \geq p_j}$ is an
647 indicator function that returns 1 if $p_i \geq p_j$ and -1 otherwise, F_{ST}^{ij} is the F_{ST} between focal
648 population i and population j, and $E\left[F_{ST}^{ij}\right]$ and $sd\left[F_{ST}^{ij}\right]$ are the expected value and standard
649 deviation of F_{ST} between populations i and j across all SNPs. We implement this polarization
650 procedure because SNP frequencies that are at an intermediate frequency in the focal
651 population, but strongly differentiated in others, can show up as strong d_i outliers in the focal
652 population due to the symmetry of F_{ST}. To identify individual eGenes and sGenes with evidence
653 of population-specific selection, we generate weighted d_i scores as described above for F_{ST}.

654

655 Due to differential levels of admixture across populations, some d_i outlier loci show genetic
656 similarity with non-African and west-African populations, suggesting that these loci are uniquely
657 differentiated in the focal population due to admixture. To eliminate candidates that may be
658 driven by admixture, we also calculate the population-branch statistic (PBS_i) [93] between each
659 focal population i and the CEU (a proxy for non-Africans) and the YRI (a proxy for sub-Saharan
660 Africans):

$$PBS_i = \frac{T^{i,YRI} + T^{i,CEU} - T^{YRI,CEU}}{2}$$

661 Where $T^{A,B} = -\log\left(1 - F_{ST}^{A,B}\right)$ and $F_{ST}^{A,B}$ is FST calculated between populations A and B. We
662 then go on to create a weighted PBS_i statistic per gene or intron as above. Candidates of

663 selection are then defined as those features with a weighted d_i and PBS_i score above the 99.5th
664 percentile of genome-wide d_i and PBS_i SNP-wise statistics.
665
666 **Declarations**
667 **Ethics approval and consent to participate**
668 Written informed consent was obtained from all participants. IRB approval for this project was
669 obtained from the University of Pennsylvania, and research/ethics approval and permits were
670 obtained from the following institutions prior to sample collection: the University of Addis Ababa
671 and the Federal Democratic Republic of Ethiopia Ministry of Science and Technology National
672 Health Research Ethics Review Committee; COSTECH, NIMR and Muhimbili University of
673 Health and Allied Sciences in Dar es Salaam, Tanzania.
674
675 **Competing interests**
676 The authors declare that they have no competing interests.
677
678 **Funding**
679 This work was supported by the grant numbers: ADA 1-19-VSN-02, and NIH grants
680 1R35GM134957, R01DK104339, and R01AR076241 to SAT. Training of DEK was
681 further supported by NIH grant T32AI007532.
682
683 **Authors' contributions**
684 SAT conceived and supervised the study. TBN, SAO, DWM, GB, WB, JBH, and AR collected
685 and processed samples. MY and SC performed SNP genotyping. CDB, GRG, RAR, RM, and
686 HL assisted in statistical and bioinformatic analysis. SR performed eQTL mapping of European-

687 Americans from GTEx. DEK performed all other analyses. DEK and SAT wrote the manuscript
688 with help from other co-authors. All authors read and approved the final manuscript.
689

690 **Acknowledgements**

691 We would like to thank all of the study participants who make this work possible, along with our
692 funding sources. We would also like to thank Dr. Nicholas Lahens and the ITMAT Bioinformatics
693 Group for their assistance in data processing.
694

695 **References**

696 1. King M-C, Wilson AC. Evolution at Two Levels in Humans and Chimpanzees. Science. 1975
697 Apr 11;188(4184):107–16.

698 2. Farh KK-H, Marson A, Zhu J, Kleinewietfeld M, Housley WJ, Beik S, et al. Genetic and
699 epigenetic fine mapping of causal autoimmune disease variants. Nature. 2015
700 Feb;518(7539):337–43.

701 3. MacArthur J, Bowler E, Cerezo M, Gil L, Hall P, Hastings E, et al. The new NHGRI-EBI
702 Catalog of published genome-wide association studies (GWAS Catalog). Nucleic Acids
703 Res. 2017 Jan 4;45(Database issue):D896–901.

704 4. Fraser HB. Gene expression drives local adaptation in humans. Genome Res. 2013
705 Jul;23(7):1089–96.

706 5. Lappalainen T. Functional genomics bridges the gap between quantitative genetics and
707 molecular biology. Genome Res. 2015 Oct;25(10):1427–31.

708 6. Popejoy AB, Fullerton SM. Genomics is failing on diversity. Nature. 2016
709 Oct;538(7624):161–4.

710 7. Sirugo G, Williams SM, Tishkoff SA. The Missing Diversity in Human Genetic Studies. Cell.
711 2019 Mar 21;177(1):26–31.

712 8. Kelly DE, Hansen MEB, Tishkoff SA. Global variation in gene expression and the value of
713 diverse sampling. Current Opinion in Systems Biology. 2017 Feb 1;1:102–8.

714 9. Fan S, Hansen MEB, Lo Y, Tishkoff SA. Going global by adapting local: A review of recent
715 human adaptation. Science. 2016 Oct 7;354(6308):54–9.

716 10. Minster RL, Hawley NL, Su C-T, Sun G, Kershaw EE, Cheng H, et al. A thrifty variant in
717 CREBRF strongly influences body mass index in Samoans. Nat Genet. 2016
718 Sep;48(9):1049–54.

11. Crawford NG, Kelly DE, Hansen MEB, Beltrame MH, Fan S, Bowman SL, et al. Loci associated with skin pigmentation identified in African populations. Science. 2017 Nov 17;358(6365):eaan8433.

12. Lappalainen T, Sammeth M, Friedländer MR, 't Hoen PAC, Monlong J, Rivas MA, et al. Transcriptome and genome sequencing uncovers functional variation in humans. Nature. 2013 Sep;501(7468):506–11.

13. Quach H, Rotival M, Pothlichet J, Loh Y-HE, Dannemann M, Zidane N, et al. Genetic Adaptation and Neandertal Admixture Shaped the Immune System of Human Populations. Cell. 2016 Oct 20;167(3):643-656.e17.

14. Nédélec Y, Sanz J, Baharian G, Szpiech ZA, Pacis A, Dumaine A, et al. Genetic Ancestry and Natural Selection Drive Population Differences in Immune Responses to Pathogens. Cell. 2016 Oct 20;167(3):657-669.e21.

15. Kwiatkowski DP. How Malaria Has Affected the Human Genome and What Human Genetics Can Teach Us about Malaria. Am J Hum Genet. 2005 Aug;77(2):171–92.

16. Tishkoff SA, Reed FA, Ranciaro A, Voight BF, Babbitt CC, Silverman JS, et al. Convergent adaptation of human lactase persistence in Africa and Europe. Nat Genet. 2007 Jan;39(1):31–40.

17. Scheinfeldt LB, Soi S, Thompson S, Ranciaro A, Woldemeskel D, Beggs W, et al. Genetic adaptation to high altitude in the Ethiopian highlands. Genome Biol. 2012;13(1):R1.

18. Yusuf AA, Govender MA, Brandenburg J-T, Winkler CA. Kidney disease and APOL1. Human Molecular Genetics. 2021 Mar 1;30(R1):R129–37.

19. Auton A, Abecasis GR, Altshuler DM, Durbin RM, Abecasis GR, Bentley DR, et al. A global reference for human genetic variation. Nature. 2015 Oct;526(7571):68–74.

20. Scheinfeldt LB, Soi S, Lambert C, Ko W-Y, Coulibaly A, Ranciaro A, et al. Genomic evidence for shared common ancestry of East African hunting-gathering populations and insights into local adaptation. PNAS. 2019 Mar 5;116(10):4166–75.

21. Tishkoff SA, Reed FA, Friedlaender FR, Ehret C, Ranciaro A, Froment A, et al. The Genetic Structure and History of Africans and African Americans. Science. 2009 May 22;324(5930):1035–44.

22. Alexander DH, Novembre J, Lange K. Fast model-based estimation of ancestry in unrelated individuals. Genome Res. 2009 Sep;19(9):1655–64.

23. Stegle O, Parts L, Piipari M, Winn J, Durbin R. Using probabilistic estimation of expression residuals (PEER) to obtain increased power and interpretability of gene expression analyses. Nat Protoc. 2012 Feb 16;7(3):500–7.

24. Newman AM, Liu CL, Green MR, Gentles AJ, Feng W, Xu Y, et al. Robust enumeration of cell subsets from tissue expression profiles. Nat Methods. 2015 May;12(5):453–7.

755 25. Glastonbury CA, Couto Alves A, El-Sayed Moustafa JS, Small KS. Cell-Type Heterogeneity
756 in Adipose Tissue Is Associated with Complex Traits and Reveals Disease-Relevant Cell-
757 Specific eQTLs. Am J Hum Genet. 2019 Jun 6;104(6):1013–24.

758 26. Zhou X, Stephens M. Genome-wide efficient mixed-model analysis for association studies.
759 Nat Genet. 2012 Jul;44(7):821–4.

760 27. Battle A, Mostafavi S, Zhu X, Potash JB, Weissman MM, McCormick C, et al. Characterizing
761 the genetic basis of transcriptome diversity through RNA-sequencing of 922 individuals.
762 Genome Res. 2013 Oct 3;gr.155192.113.

763 28. THE GTEX CONSORTIUM. The GTEx Consortium atlas of genetic regulatory effects across
764 human tissues. Science. 2020 Sep 11;369(6509):1318–30.

765 29. Ye CJ, Feng T, Kwon H-K, Raj T, Wilson MT, Asinovski N, et al. Intersection of population
766 variation and autoimmunity genetics in human T cell activation. Science. 2014 Sep
767 12;345(6202):1254665.

768 30. Zanetti D, Weale ME. Transethnic differences in GWAS signals: A simulation study. Ann
769 Hum Genet. 2018 Sep;82(5):280–6.

770 31. Ongen H, Buil A, Brown AA, Dermitzakis ET, Delaneau O. Fast and efficient QTL mapper
771 for thousands of molecular phenotypes. Bioinformatics. 2016 May 15;32(10):1479–85.

772 32. Võsa U, Claringbould A, Westra H-J, Bonder MJ, Deelen P, Zeng B, et al. Large-scale cis-
773 and trans-eQTL analyses identify thousands of genetic loci and polygenic scores that
774 regulate blood gene expression. Nat Genet. 2021 Sep;53(9):1300–10.

775 33. Tehranchi A, Hie B, Dacre M, Kaplow I, Pettie K, Combs P, et al. Fine-mapping cis-
776 regulatory variants in diverse human populations. Morris AP, Wittkopp PJ, editors. eLife.
777 2019 Jan 16;8:e39595.

778 34. Dunham I, Kundaje A, Aldred SF, Collins PJ, Davis CA, Doyle F, et al. An integrated
779 encyclopedia of DNA elements in the human genome. Nature. 2012 Sep;489(7414):57–74.

780 35. International Multiple Sclerosis Genetics Consortium. Multiple sclerosis genomic map
781 implicates peripheral immune cells and microglia in susceptibility. Science. 2019 Sep
782 27;365(6460):eaav7188.

783 36. Lill CM, Luessi F, Alcina A, Sokolova EA, Ugidos N, de la Hera B, et al. Genome-wide
784 significant association with seven novel multiple sclerosis risk loci. J Med Genet. 2015
785 Dec;52(12):848–55.

786 37. Enattah NS, Sahi T, Savilahti E, Terwilliger JD, Peltonen L, Järvelä I. Identification of a
787 variant associated with adult-type hypolactasia. Nat Genet. 2002 Feb;30(2):233–7.

788 38. Hamblin MT, Di Rienzo A. Detection of the signature of natural selection in humans:
789 evidence from the Duffy blood group locus. Am J Hum Genet. 2000 May;66(5):1669–79.

790 39. Kudaravalli S, Veyrieras J-B, Stranger BE, Dermitzakis ET, Pritchard JK. Gene expression
791 levels are a target of recent natural selection in the human genome. Mol Biol Evol. 2009
792 Mar;26(3):649–58.

793 40. Shaheen R, Alsahli S, Ewida N, Alzahrani F, Shamseldin HE, Patel N, et al. Biallelic
794 Mutations in Tetratricopeptide Repeat Domain 26 (Intraflagellar Transport 56) Cause
795 Severe Biliary Ciliopathy in Humans. Hepatology. 2020 Jun;71(6):2067–79.

796 41. Mahajan A, Go MJ, Zhang W, Below JE, Gaulton KJ, Ferreira T, et al. Genome-wide trans-
797 ancestry meta-analysis provides insight into the genetic architecture of type 2 diabetes
798 susceptibility. Nat Genet. 2014 Mar;46(3):234–44.

799 42. Heaton MP, Clawson ML, Chitko-Mckown CG, Leymaster KA, Smith TPL, Harhay GP, et al.
800 Reduced lentivirus susceptibility in sheep with TMEM154 mutations. PLoS Genet. 2012
801 Jan;8(1):e1002467.

802 43. Baggiolini M, Dewald B, Moser B. Interleukin-8 and related chemotactic cytokines--CXC and
803 CC chemokines. Adv Immunol. 1994;55:97–179.

804 44. Revez JA, Lin T, Qiao Z, Xue A, Holtz Y, Zhu Z, et al. Genome-wide association study
805 identifies 143 loci associated with 25 hydroxyvitamin D concentration. Nat Commun. 2020
806 Apr 2;11(1):1647.

807 45. Rhodes DA, Reith W, Trowsdale J. Regulation of Immunity by Butyrophilins. Annu Rev
808 Immunol. 2016 May 20;34:151–72.

809 46. Hirschhorn R, Huie ML, Kasper JS. Computer assisted cloning of human neutral α-
810 glucosidase C (GANC): A new paralog in the glycosyl hydrolase gene family 31. Proc Natl
811 Acad Sci U S A. 2002 Oct 15;99(21):13642–6.

812 47. Akey JM, Ruhe AL, Akey DT, Wong AK, Connelly CF, Madeoy J, et al. Tracking footprints of
813 artificial selection in the dog genome. PNAS. 2010 Jan 19;107(3):1160–5.

814 48. Yi X, Liang Y, Huerta-Sanchez E, Jin X, Cuo ZXP, Pool JE, et al. Sequencing of 50 human
815 exomes reveals adaptation to high altitude. Science. 2010 Jul 2;329(5987):75–8.

816 49. Shang L, Smith JA, Zhao W, Kho M, Turner ST, Mosley TH, et al. Genetic Architecture of
817 Gene Expression in European and African Americans: An eQTL Mapping Study in
818 GENOA. Am J Hum Genet. 2020 Apr 2;106(4):496–512.

819 50. Storey JD, Madeoy J, Strout JL, Wurfel M, Ronald J, Akey JM. Gene-expression variation
820 within and among human populations. Am J Hum Genet. 2007 Mar;80(3):502–9.

821 51. Idaghdour Y, Storey JD, Jadallah SJ, Gibson G. A genome-wide gene expression signature
822 of environmental geography in leukocytes of Moroccan Amazighs. PLoS Genet. 2008 Apr
823 11;4(4):e1000052.

824 52. Ferreira PG, Muñoz-Aguirre M, Reverter F, Sá Godinho CP, Sousa A, Amadoz A, et al. The
825 effects of death and post-mortem cold ischemia on human tissue transcriptomes. Nat
826 Commun. 2018 Feb 13;9(1):490.

827 53. Marigorta UM, Navarro A. High Trans-ethnic Replicability of GWAS Results Implies
828 Common Causal Variants. PLOS Genetics. 2013 Jun 13;9(6):e1003566.

829 54. Li YR, Keating BJ. Trans-ethnic genome-wide association studies: advantages and
830 challenges of mapping in diverse populations. Genome Medicine. 2014 Oct 31;6(10):91.

831 55. Brown BC, Asian Genetic Epidemiology Network Type 2 Diabetes Consortium, Ye CJ, Price
832 AL, Zaitlen N. Transethnic Genetic-Correlation Estimates from Summary Statistics. Am J
833 Hum Genet. 2016 Jul 7;99(1):76–88.

834 56. Gabriel SB, Schaffner SF, Nguyen H, Moore JM, Roy J, Blumenstiel B, et al. The structure
835 of haplotype blocks in the human genome. Science. 2002 Jun 21;296(5576):2225–9.

836 57. Sawyer SL, Mukherjee N, Pakstis AJ, Feuk L, Kidd JR, Brookes AJ, et al. Linkage
837 disequilibrium patterns vary substantially among populations. Eur J Hum Genet. 2005
838 May;13(5):677–86.

839 58. Reich DE, Cargill M, Bolk S, Ireland J, Sabeti PC, Richter DJ, et al. Linkage disequilibrium in
840 the human genome. Nature. 2001 May;411(6834):199–204.

841 59. Jakobsson M, Scholz SW, Scheet P, Gibbs JR, VanLiere JM, Fung H-C, et al. Genotype,
842 haplotype and copy-number variation in worldwide human populations. Nature. 2008
843 Feb;451(7181):998–1003.

844 60. Quach H, Rotival M, Pothlichet J, Loh Y-HE, Dannemann M, Zidane N, et al. Genetic
845 Adaptation and Neandertal Admixture Shaped the Immune System of Human Populations.
846 Cell. 2016 Oct;167(3):643-656.e17.

847 61. Stranger BE, Forrest MS, Dunning M, Ingle CE, Beazley C, Thorne N, et al. Relative Impact
848 of Nucleotide and Copy Number Variation on Gene Expression Phenotypes. Science. 2007
849 Feb 9;315(5813):848–53.

850 62. Stranger BE, Montgomery SB, Dimas AS, Parts L, Stegle O, Ingle CE, et al. Patterns of Cis
851 Regulatory Variation in Diverse Human Populations. PLOS Genetics. 2012 Apr
852 19;8(4):e1002639.

853 63. Valente EM, Logan CV, Mougou-Zerelli S, Lee JH, Silhavy JL, Brancati F, et al. Mutations in
854 TMEM216 perturb ciliogenesis and cause Joubert, Meckel and related syndromes. Nat
855 Genet. 2010 Jul;42(7):619–25.

856 64. Lee JH, Silhavy JL, Lee JE, Al-Gazali L, Thomas S, Davis EE, et al. Evolutionarily
857 assembled cis-regulatory module at a human ciliopathy locus. Science. 2012 Feb
858 24;335(6071):966–9.

859 65. Choi H, Shin JH, Kim ES, Park SJ, Bae I-H, Jo YK, et al. Primary Cilia Negatively Regulate
860 Melanogenesis in Melanocytes and Pigmentation in a Human Skin Model. PLoS One.
861 2016;11(12):e0168025.

862 66. Guan J, Gupta R, Filipp FV. Cancer systems biology of TCGA SKCM: Efficient detection of
863 genomic drivers in melanoma. Sci Rep. 2015 Jan 20;5(1):7857.

67. Kundaje A, Meuleman W, Ernst J, Bilenky M, Yen A, Heravi-Moussavi A, et al. Integrative analysis of 111 reference human epigenomes. Nature. 2015 Feb;518(7539):317–30.

68. Cuomo ASE, Seaton DD, McCarthy DJ, Martinez I, Bonder MJ, Garcia-Bernardo J, et al. Single-cell RNA-sequencing of differentiating iPS cells reveals dynamic genetic effects on gene expression. Nat Commun. 2020 Feb 10;11(1):810.

69. Ward MC, Banovich NE, Sarkar A, Stephens M, Gilad Y. Dynamic effects of genetic variation on gene expression revealed following hypoxic stress in cardiomyocytes. Stegle O, Wittkopp PJ, editors. eLife. 2021 Feb 8;10:e57345.

70. Raj T, Rothamel K, Mostafavi S, Ye C, Lee MN, Replogle JM, et al. Polarization of the effects of autoimmune and neurodegenerative risk alleles in leukocytes. Science. 2014 May 2;344(6183):519–23.

71. Randolph HE, Fiege JK, Thielen BK, Mickelson CK, Shiratori M, Barroso-Batista J, et al. Genetic ancestry effects on the response to viral infection are pervasive but cell type specific. Science. 2021 Nov 26;374(6571):1127–33.

72. Neavin D, Nguyen Q, Daniszewski MS, Liang HH, Chiu HS, Wee YK, et al. Single cell eQTL analysis identifies cell type-specific genetic control of gene expression in fibroblasts and reprogrammed induced pluripotent stem cells. Genome Biology. 2021 Mar 5;22(1):76.

73. Browning SR, Browning BL. Rapid and Accurate Haplotype Phasing and Missing-Data Inference for Whole-Genome Association Studies By Use of Localized Haplotype Clustering. Am J Hum Genet. 2007 Nov;81(5):1084–97.

74. Das S, Forer L, Schönherr S, Sidore C, Locke AE, Kwong A, et al. Next-generation genotype imputation service and methods. Nat Genet. 2016 Oct;48(10):1284–7.

75. Manichaikul A, Mychaleckyj JC, Rich SS, Daly K, Sale M, Chen W-M. Robust relationship inference in genome-wide association studies. Bioinformatics. 2010 Nov 15;26(22):2867–73.

76. Chang CC, Chow CC, Tellier LC, Vattikuti S, Purcell SM, Lee JJ. Second-generation PLINK: rising to the challenge of larger and richer datasets. Gigascience. 2015;4:7.

77. Patterson N, Price AL, Reich D. Population Structure and Eigenanalysis. PLOS Genetics. 2006 Dec 22;2(12):e190.

78. Alexander DH, Lange K. Enhancements to the ADMIXTURE algorithm for individual ancestry estimation. BMC Bioinformatics. 2011 Jun 18;12(1):246.

79. Altschul SF, Gish W, Miller W, Myers EW, Lipman DJ. Basic local alignment search tool. J Mol Biol. 1990 Oct 5;215(3):403–10.

80. Dobin A, Davis CA, Schlesinger F, Drenkow J, Zaleski C, Jha S, et al. STAR: ultrafast universal RNA-seq aligner. Bioinformatics. 2013 Jan 1;29(1):15–21.

81. Frankish A, Diekhans M, Ferreira A-M, Johnson R, Jungreis I, Loveland J, et al. GENCODE reference annotation for the human and mouse genomes. Nucleic Acids Research. 2019 Jan 8;47(D1):D766–73.

82. Liao Y, Smyth GK, Shi W. featureCounts: an efficient general purpose program for assigning sequence reads to genomic features. Bioinformatics. 2014 Apr 1;30(7):923–30.

83. Li B, Dewey CN. RSEM: accurate transcript quantification from RNA-Seq data with or without a reference genome. BMC Bioinformatics. 2011 Aug 4;12(1):323.

84. Li YI, Knowles DA, Humphrey J, Barbeira AN, Dickinson SP, Im HK, et al. Annotation-free quantification of RNA splicing using LeafCutter. Nat Genet. 2018 Jan;50(1):151–8.

85. Abbas AR, Wolslegel K, Seshasayee D, Modrusan Z, Clark HF. Deconvolution of blood microarray data identifies cellular activation patterns in systemic lupus erythematosus. PLoS One. 2009 Jul 1;4(7):e6098.

86. Giambartolomei C, Vukcevic D, Schadt EE, Franke L, Hingorani AD, Wallace C, et al. Bayesian Test for Colocalisation between Pairs of Genetic Association Studies Using Summary Statistics. PLOS Genetics. 2014 May 15;10(5):e1004383.

87. Maller JB, McVean G, Byrnes J, Vukcevic D, Palin K, Su Z, et al. Bayesian refinement of association signals for 14 loci in 3 common diseases. Nat Genet. 2012 Dec;44(12):1294–301.

88. McLaren W, Gil L, Hunt SE, Riat HS, Ritchie GRS, Thormann A, et al. The Ensembl Variant Effect Predictor. Genome Biology. 2016 Jun 6;17(1):122.

89. liftOver [Internet]. Bioconductor. [cited 2021 Nov 24]. Available from: http://bioconductor.org/packages/liftOver/

90. Storey JD, Bass AJ, Dabney A, Robinson D, Warnes G. qvalue: Q-value estimation for false discovery rate control [Internet]. Bioconductor version: Release (3.14); 2021 [cited 2021 Nov 24]. Available from: https://bioconductor.org/packages/qvalue/

91. The GTEx Consortium. The GTEx Consortium atlas of genetic regulatory effects across human tissues. Science. 2020 Sep 11;369(6509):1318–30.

92. Bhatia G, Patterson N, Sankararaman S, Price AL. Estimating and interpreting FST: The impact of rare variants. Genome Res. 2013 Sep 1;23(9):1514–21.

93. Yi X, Liang Y, Huerta-Sanchez E, Jin X, Cuo ZXP, Pool JE, et al. Sequencing of 50 Human Exomes Reveals Adaptation to High Altitude. Science. 2010 Jul 2;329(5987):75–8.

94. Kent WJ, Sugnet CW, Furey TS, Roskin KM, Pringle TH, Zahler AM, et al. The human genome browser at UCSC. Genome Res. 2002 Jun;12(6):996–1006.

95. Ernst J, Kellis M. ChromHMM: automating chromatin-state discovery and characterization. Nat Methods. 2012 Mar;9(3):215–6.

96. Liu B, Gloudemans MJ, Rao AS, Ingelsson E, Montgomery SB. Abundant associations with gene expression complicate GWAS follow-up. Nat Genet. 2019 May;51(5):768–9.

Figures

Figure 1: Global and genetic structure of study populations

A) Locations of East African populations sampled in this study across Ethiopia and Tanzania. **B)** Principal Component Analysis of genetic data across 162 East Africans, combined with 20 West African Yoruba (YRI), 20 European Americans (CEU), and 20 Han Chinese (CHB) from the 1000 Genomes Project. **C)** ADMIXTURE analysis of East African, YRI, CEU, and CHB populations.

Figure 2: Genomic context of tQTLs

A) Enrichment of top eQTLs near the transcription start site (TSS) of their target gene. **B)** Enrichment of top sQTLs near the intron boundary of their target intron. Densities of sQTLs are separated depending on whether they're upstream of the target intron (5' distance), within the intron (intron fraction), or downstream of the intron (3' distance). **C)** Enrichment of tQTLs across functional categories, stratified by FDR significance and posterior probability (PP) of being causal. Categories include chromatin accessibility QTLs (caQTL) in LCLs from Tehranchi *et al.* [33]; transcription factor binding sites (TFBS) for 140 transcription factors in GM12878 LCLs [34]; transcription start sites (TSS), enhancers (Enh), Polycomb-repressed chromatin (ReprPC), transcribed (Tx), and heterochromatin (Het) annotations from ChromHMM in GM12878 LCLs [34]; and 3' UTR, 5' UTR, intron, splice site, synonymous, missense, and start gain/loss or stop gain/loss annotations from Variant Effect Predictor (VEP) [88].

Figure 3: Replication of tQTLs between East Africans and GTEx v8

A) Minor allele frequency distribution in GTEx v8 of FDR-significant tQTLs identified in East Africans, colored by whether they have a p-value less than 0.01 in GTEx v8. **B)** Comparison effect sizes of tQTLs identified in East Africans. Lines show the best fit regression line between

East Africans and GTEx v8 effect sizes, colored by whether the tQTL is shared (i.e. is no longer significant after conditioning) or is independent (remains significant after conditioning).

Figure 4: Fine mapping in East Africans vs. GTEx v8

A) Credible set (CS) sizes for eGenes identified in 162 East Africans (Afr) or a subset of 162 European Americans from GTEx v8 (EA162). Points are colored by the fraction of SNPs in the smaller credible set A that are shared with the larger set B, 1 indicating that the smaller set is a subset of the larger set, and 0 indicating the smaller set shares no SNPs with the larger set. **B)** Locus plot of *NR1D1* eQTLs identified in 162 East Africans (Afr) or the full GTEx v8 cohort (v8). P-values are overlaid with African (YRI) and European-American (CEU) recombination rates, GENCODE v19 [81] gene models from the UCSC genome browser [94] (*http://genome.ucsc.edu*) and inferred ChromHMM[95] states for GM12878 [34]. The top SNP in Africans, rs883871, disrupts a nucleotide for the core motif of ETS-family transcription factors (motif of *ETS1* shown).

Figure 5: Population-specific selection in East Africa.

A) Gene scores for the *d*-statistics plotted against the population branch statistics (*PBS*) for each population. *PBS* is calculated for each focal population versus the CEU and YRI populations from the 1000 Genomes Project. Genes with a score above the 99.5th percentile of genome-wide statistics for *d* and *PBS* are highlighted in red. **B)** Comparison of pigmentation GWAS p-values from Crawford *et al*. [11] against eQTL p-values from our study (East Africa), GTEx v8 Whole Blood, or GTEx v8 Sun-exposed skin (lower leg), in the style of LocusCompare [96]. Variants are colored by their degree of LD with three top pigmentation GWAS variants, rs7948623, rs11230664, and rs2512809. Colocalization probabilities from *coloc* [86] (PP4) are indicated for each eQTL group.

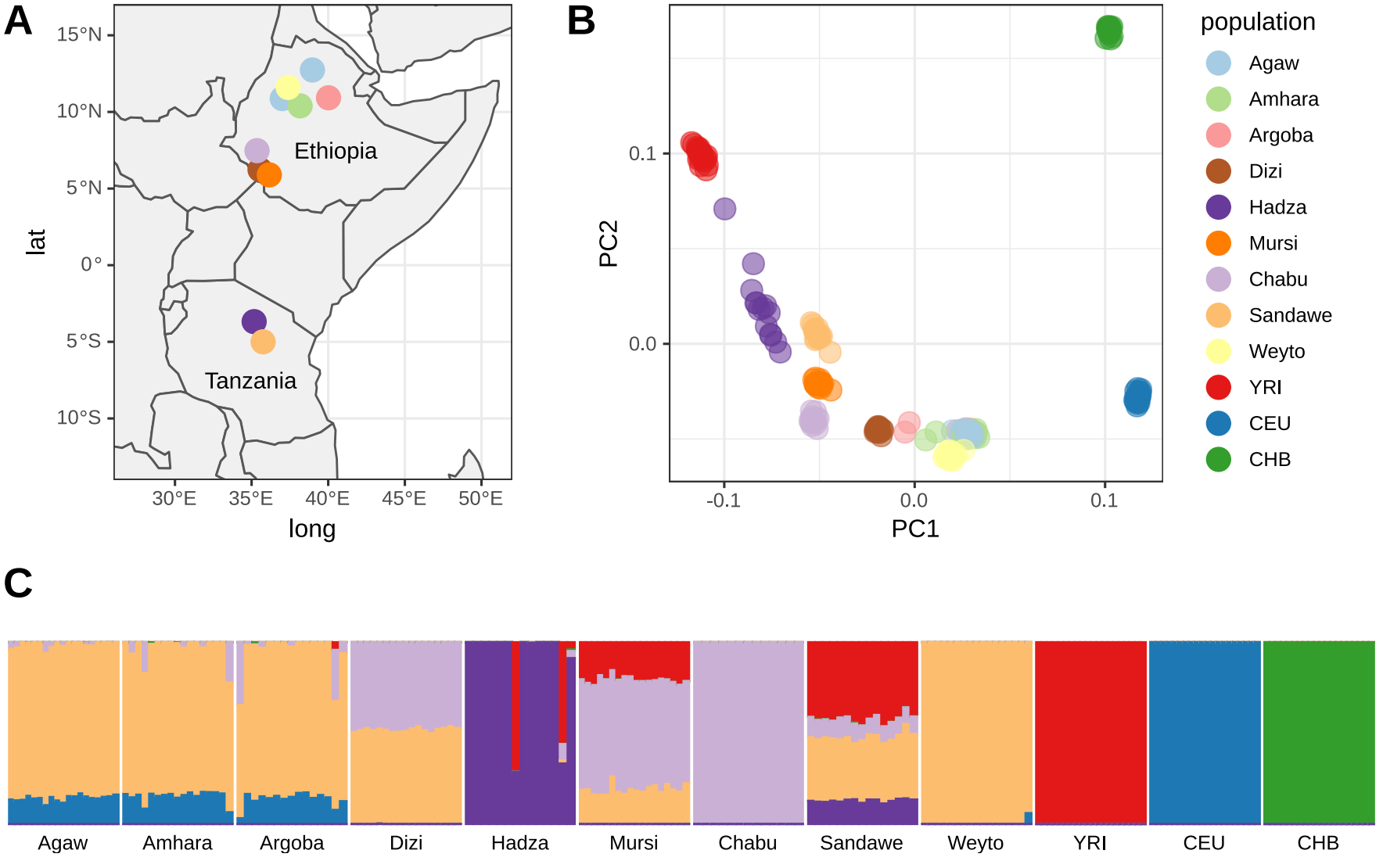
A
15°N
10°N
5°N
0°
5°S
10°S
lat
Ethiopia
Tanzania
30°E
35°E
40°E
45°E
50°E
long
B
PC2
0.1
0.0
-0.1
0.0
0.1
PC1
population
Agaw
Amhara
Argoba
Dizi
Hadza
Mursi
Chabu
Sandawe
Weyto
YRI
CEU
CHB
C
Agaw
Amhara
Argoba
Dizi
Hadza
Mursi
Chabu
Sandawe
Weyto
YRI
CEU
CHB

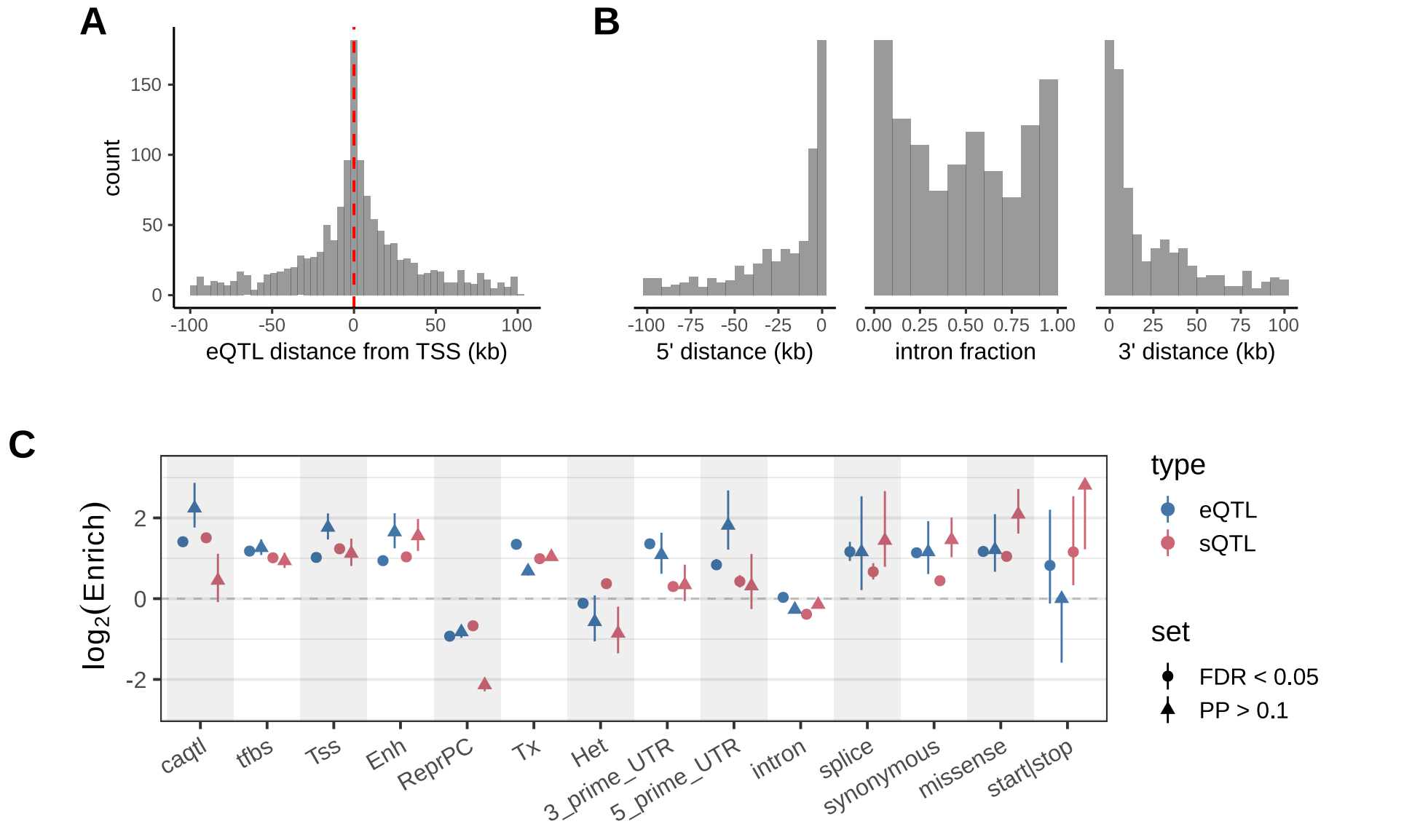
A
count
150
100
50
0
-100
-50
0
50
100
eQTL distance from TSS (kb)
B
-100 -75 -50 -25 0
5' distance (kb)
0.00 0.25 0.50 0.75 1.00
intron fraction
0 25 50 75 100
3' distance (kb)
C
log2(Enrich)
2
0
-2
caqtl
tfbs
Tss
Enh
ReprPC
Tx
Het
3_prime_UTR
5_prime_UTR
intron
splice
synonymous
missense
start|stop
type
eQTL
sQTL
set
FDR < 0.05
PP > 0.1

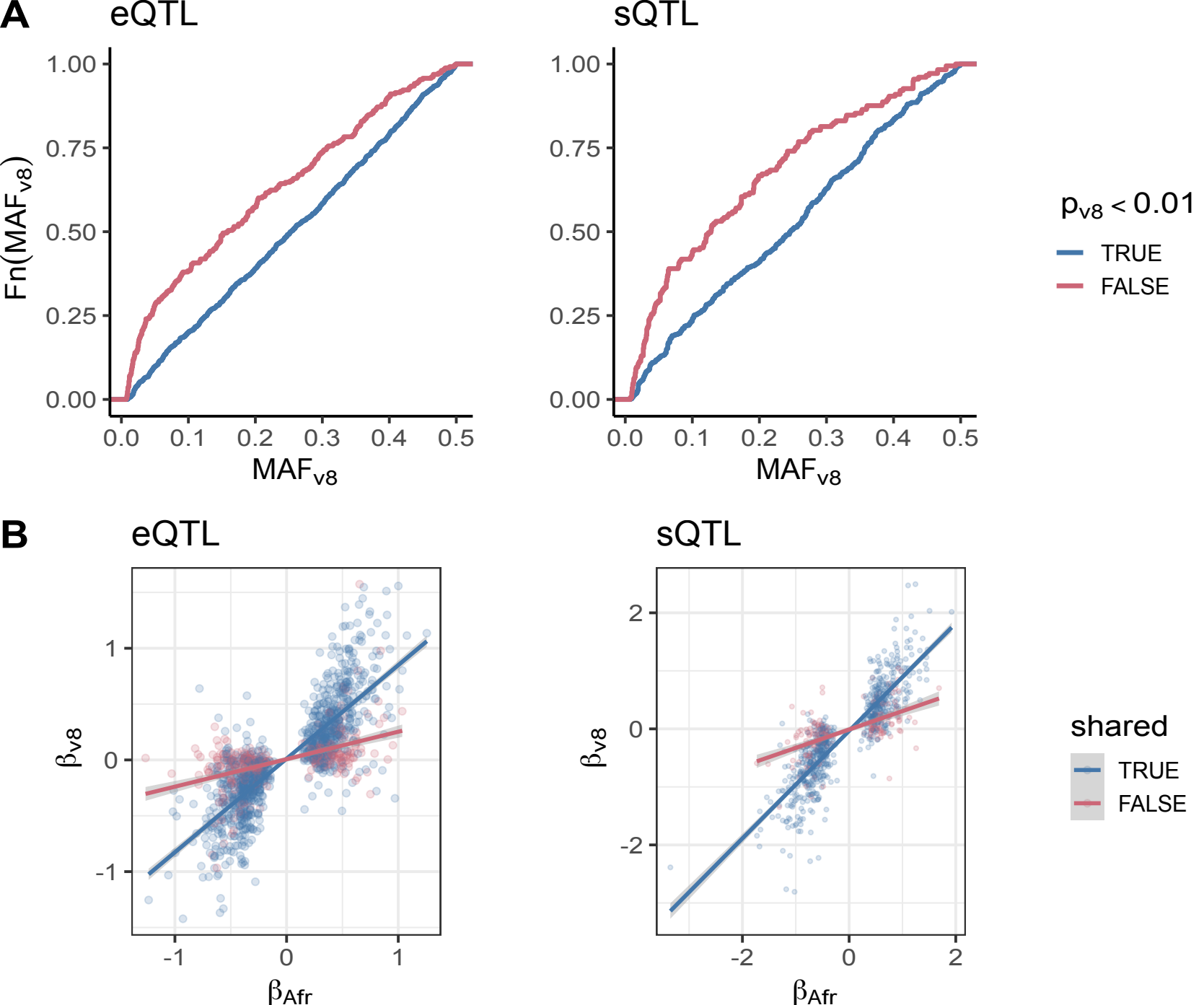
A
eQTL
sQTL
1.00
0.75
0.50
0.25
0.00
Fn(MAF_v8)
0.0
0.1
0.2
0.3
0.4
0.5
MAF_v8
p_v8 < 0.01
TRUE
FALSE
B
eQTL
sQTL
β_v8
β_Afr
shared
TRUE
FALSE

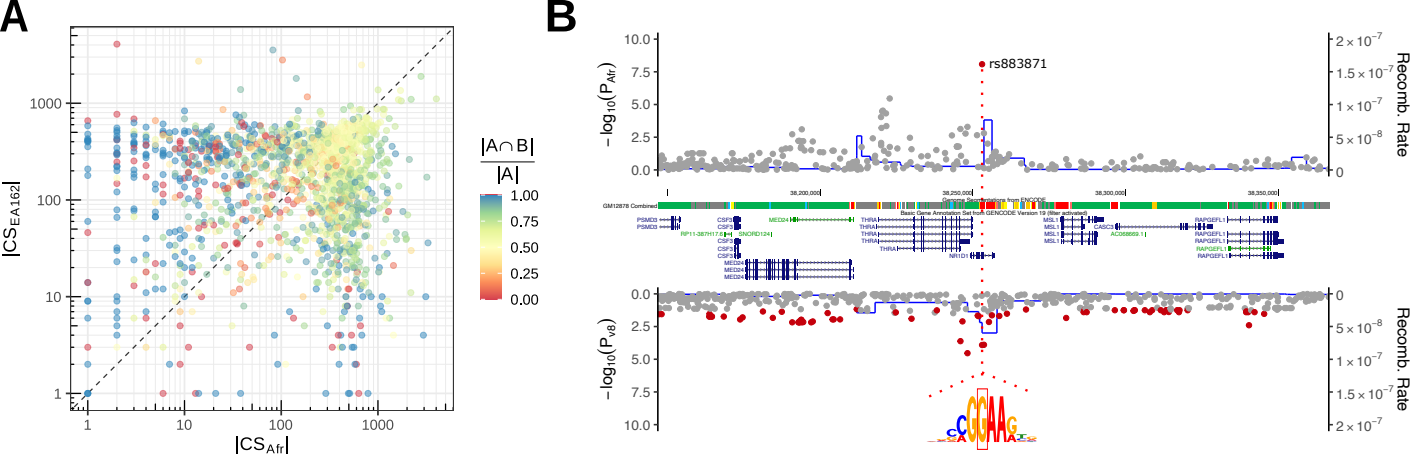
A
|CS_EA162|
|CS_Afr|
1
10
100
1000
|A∩B| / |A|
1.00
0.75
0.50
0.25
0.00
B
−log10(P_Afr)
rs883871
Recomb. Rate
−log10(P_v8)
GM12878 Combined
Basic Gene Annotation Set from GENCODE Version 19 (liftover activated)
PSMD3
CSF2RB
MED24
THRA
NR1D1
MSL1
CASC8
AC068650.1
RAPGEFL1